Hot-electron effects in strongly localized doped silicon at low temperature

M. Galeazzi,* D. Liu, D. McCammon, L. E. Rocks, W. T. Sanders, B. Smith, P. Tan, and J. E. Vaillancourt
Physics Department, University of Wisconsin, 1150 University Avenue, Madison, Wisconsin 53706, USA

K. R. Boyce, R. P. Brekosky, J. D. Gygax, R. L. Kelley, C. A. Kilbourne, F. S. Porter, and C. M. Stahle
NASA/Goddard Space Flight Center, Mailstop 662, Greenbelt, Maryland 20771, USA

A. E. Szymkowiak
Physics Department, Yale University, P.O. Box 208121, New Haven, Connecticut 06520, USA
(Received 26 June 2007; published 18 October 2007)

The electrical conductivity in doped semiconductors in the strongly localized variable range hopping regime is currently explained as phonon-assisted electron hopping. While investigating the non-Ohmic behavior of doped silicon at temperatures of 0.05–1 K, we found strong evidence for the existence of separate temperatures for the electron and phonon systems analogous to the hot-electron effect in metals. This behavior cannot easily be explained by phonon-assisted hopping and seems to favor instead a direct electron-electron interaction at low temperature. A hot-electron model makes definite predictions for the dependence of the electrical conductivity on the bias power, the frequency dependence of the resistance nonlinearities, and for an additional noise term. We have made a systematic investigation of these quantities, and find all of them in good agreement with the model predictions over a wide range of parameters.

DOI: 10.1103/PhysRevB.76.155207 PACS number(s): 63.20.Kr, 72.20.−i, 61.72.Tt

I. INTRODUCTION

Doped silicon and germanium have long been employed in the strongly localized variable range hopping (VRH) regime to make sensitive thermometers for low-temperature bolometers and calorimeters. The performance of these devices is severely limited by the electrical nonlinearity, or voltage dependence, of the resistance. Hopping conductivity is expected to be nonlinear, with an exponential dependence on the electric field.[1,2] However, it has been noted for some time that for most combinations of temperature and doping density of interest for detectors, the functional form of this nonlinearity is quite different from these theoretical predictions. It can instead be well described by a hot-electron model, where the resistance is a function only of the "electron temperature," and the bias power must reach the phonon system through an electron-phonon thermal resistance with a well-defined power law temperature dependence.[3,4] This behavior is quite analogous to that expected and observed for diffuse conductivity in metallic systems, but it would in fact be quite remarkable if this were more than a convenient empirical description for these VRH systems, which are far on the insulating side of the metal-insulator transition and have strongly localized electrons. Long-range Coulomb interactions shift the energy of individual local states depending on which others are occupied, but there is still a discrete set of possible energies. In VRH theory, the arbitrary amounts of energy required to shift electrons to a new set of discrete locations are provided by the delocalized phonon system, which has an essentially continuous energy distribution. Enabling the electrons to establish their own equilibrium independent of the phonon system requires that electron energy be available from a continuous, and therefore presumably delocalized, system.

A similar behavior has been observed in two-dimensional (2D) systems[5,6] in the VRH regime. It has been recently suggested that in such 2D systems diffuse conductivity of electrons is, in fact, relevant over a much larger range of electrical conductivities than previously thought, due to interference between electron channels.[7,8] However, the 2D systems investigated have significant differences compared with more traditional three-dimensional VRH conductivity and the combination of localized electrons and delocalized electron energy would not appear to be explained by any current theory. For such a departure from accepted theory, one would like to have better evidence than the perhaps fortuitous fit to a particular functional form for $R(T,E)$. Marnieros *et al.*[9] have made simultaneous measurement of the apparent electron-phonon thermal conductivity $G_{e\text{-ph}}$, the electron-phonon coupling time $\tau_{e\text{-ph}}$, and the total heat capacity C in amorphous Nb_xSi_{1-x}. They find that the derived heat capacity of the electron system, $C_e = G_{e\text{-ph}} \times \tau_{e\text{-ph}}$, agrees well with the total measured C after subtracting the lattice heat capacity, provided that the resistance is a function only of the electron temperature. This led them to question the assumption of phonon-assisted hopping, and to suggest that direct electron-electron assisted hopping might dominate at low temperatures.

We have made similar independent measurements of $G_{e\text{-ph}}$, $\tau_{e\text{-ph}}$, and $C_{\text{total}} - C_{\text{lattice}}$ for Si:P:B, and also find good agreement of $G_{e\text{-ph}} \times \tau_{e\text{-ph}}$ and $C - C_{\text{lattice}}$ for this doped crystalline semiconductor system. We go one step farther, and note that if we can indeed regard this as a two-bath thermodynamic system, then we expect fluctuations of the electron temperature T_e caused by random exchange of energy between the electron and phonon systems, which should in turn produce fluctuations in the resistance $R(T_e)$. Measurements of the voltage noise indeed show an excess above Johnson noise. Over a wide range of bias power and temperature, this excess is in good agreement with the predictions of standard bolometer theory when the effects of electrothermal feed-

 ©2007 The American Physical Society

back are included.[10,11] This appears to support the physical reality of a distinct electron temperature, with whatever implications this might have.

II. EXPERIMENT

The devices tested in this experiment are ion implanted and diffused n-type Si:P:B, 50% compensated, with doped dimensions $100\times120\times1.4\ \mu\text{m}^3$. The devices have been fabricated using the deep implant and oxide-bounded diffusion technique[12,13] that guarantees good uniformity of the implant and a well defined doping volume.

Several Si:P:B devices with net doping density ranging from 2.4×10^{18} to $2.8\times10^{18}\ \text{cm}^3$ have been fabricated and tested.[13] The critical density for this 50% compensated system is estimated to be[14] $2.85\times10^{18}\ \text{cm}^{-3}$. The thermistors are implanted in the 1.4 μm device layer of a 60 ohm cm silicon on insulator (SOI) wafer, then annealed at 1175 °C in dry N_2 for 12 h while the buried oxide and a capping oxide layer confine the dopant diffusion. This high-temperature annealing step diffuses the implant throughout the depth of the top layer of the SOI wafer. Degenerate contact bars are then implanted across the 120 μm width on two sides of the thermistor extending through most of the 1.4 μm thickness. Narrow degenerate traces are implanted between these contact bars and the bonding pads. The capping oxide is removed and a deep reactive ion etch (DRIE) through the device layer is used to sharply define the edges of the thermistor. More fabrication detail can be found in Brekoski *et al.*[13]

For this and the following measurements (unless otherwise specified), the devices are heat sunk to the cold plate of an adiabatic demagnetization refrigerator (ADR) using GE varnish. The devices are biased through 90 MΩ load resistors mounted on the ADR cold plate and the voltage across the devices is read through junction field effect transistor (JFET) source followers located nearby and operating at 120 K, then amplified by a room-temperature stage.[15] The total noise of the readout system is less than $4\ \text{nV}/\sqrt{Hz}$ across the 1 Hz to 10 kHz frequency range. The load resistors are composed of three 30 MΩ nichrome thin film chip resistors manufactured by Mini-Systems, Inc.[15]

The resistance versus temperature data in the low-frequency, low-power limit show the behavior expected for VRH with a Coulomb gap

$$R = R_0 e^{\sqrt{T_0/T}}, \tag{1}$$

with the usual upward deviation[16] for $T_0/T > 2.4$. Values of T_0 range from about 3 to 20 K. More extensive data on $R(T)$ of similar, but thinner, devices can be found in Ref. 16.

III. THERMAL CONDUCTIVITY BETWEEN ELECTRON AND PHONONS

To measure the thermal conductivity between electron and phonon systems, we measure the current versus voltage curves at various values of the cold plate temperature. The analysis assumed that the electron system has its own temperature, T_e, decoupled from the lattice phonon system with temperature T_{ph}, and that the resistance is a function only of T_e (the resistance depends also on the electric field E, but this can be neglected for the range of doping densities and fields used here[4]). Bias power is assumed to be dissipated in the electron system distributed among the electrons involved in conduction to establish a temperature independent of the lattice phonon system. In steady state, this power is then conducted to the lattice through a thermal conductivity $G_{e\text{-ph}}$ that is assumed to have a power-law temperature dependence

$$G_{e\text{-ph}} = G_0 T^{\beta}. \tag{2}$$

This apparent thermal conductivity is easily evaluated by measuring the resistance of the samples as a function of the electrical power. The strong heat sinking keeps the phonon system at the temperature of the cold plate. The electron system is heated by the applied electrical bias power and, as a consequence, the resistance should drop at higher powers.[11] Starting from the definition of thermal conductivity ($G \equiv dP/dT$) and Eq. (2), we can integrate the differential equation between the phonon temperature and the electron temperature to obtain a relation between the electron temperature, the phonon temperature, and the electrical bias

$$(T_e^{\beta+1} - T_{\text{ph}}^{\beta+1}) = \frac{\beta+1}{G_0} P, \tag{3}$$

where $P = IV$ is the dissipated power. From Eq. (3) we can then obtain an expression for the electron temperature as a function of the phonon temperature and the electrical power, which can be used in Eq. (1) to obtain an expression for the device resistance as a function of the phonon temperature and the electrical power $R(T_{\text{ph}}, P)$.

Since the $R(T_e)$ function can be measured directly in the low-power limit where T_e is very close to T_{lattice}, this model has only two free parameters, which are the G_0 and β of the electron-phonon "thermal conductance." The resistance of a second doped region on the same small silicon die can be monitored with low bias power to ensure that the lattice temperature does not increase as power is applied to the test device.

Figure 1 shows a typical measurement of the resistance as a function of the applied power for several heat sink temperatures and the corresponding fit using a hot-electron model. The results of such fits over a wide range of lattice temperature and power are consistent with those of Zhang *et al.*[4] with a uniform decrease of about 40% in the conductance per unit volume, which is probably due to the uncertainty in determining the effective volume in their much thinner implanted devices. All these devices show a rather precise power-law behavior of the apparent thermal conductivity. The exponent β is constant with temperature, but changes from about 4.3 to 5.8 as the doping density is varied over a wide range.[14]

In standard VRH theory, an exponential dependence of the device resistance on the electric field in the samples is expected.[1,2] It was, however, impossible to obtain a good fit of the data with such a field effect model. The best fit χ^2 is systematically at least an order of magnitude larger than for fits with the hot-electron model. The dotted lines of Fig. 1

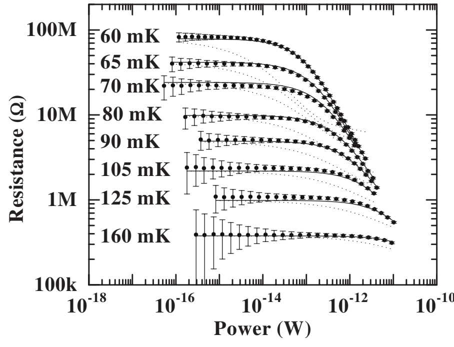

FIG. 1. Typical resistance versus power curves for an implanted silicon thermistor cemented directly to a heat sink, so that the lattice temperature is equal to the heat sink temperature (given on the left). For this device the net doping density is 2.6×10^{18} cm^{-3}. The electric field is about 600 V/m for a power of 10^{-14} W at 60 mK. The data have been acquired at different heat sink temperatures, ranging from 60 to 160 mK. The solid lines are the best fit to the hot-electron model. The dotted lines are the best fit to the field effect model [see Eq. (4)]. The best fit parameters are $R_0=320\ \Omega$, $T_0=8.55$ K, $G(0.1\text{ K})=1.43\times10^{-10}$ W K^{-1} (hot-electron model), $\beta=4.68\pm0.03$ (hot-electron model), and $Ca=7.72\times10^{-8}$ m (field-effect model).

represent the best fit of the data to the field effect model. For this fit we varied Ca in the expression derived in Zhang *et al.*:[16]

$$R(T_e,E)=R(T_e,0)\exp\left(\frac{e}{k}\frac{Ca\sqrt{T_0}}{2}\frac{E}{T_e^{3/2}}\right),\qquad(4)$$

where E is the electric field, e is the electron charge, k is Boltzmann's constant, C is a constant of the order of unity, and a is the localization radius.

IV. ELECTRON HEAT CAPACITY

The hot-electron model makes additional predictions that can be investigated experimentally.[11] First, if we assume that the electron system has a finite heat capacity C_e, we expect to see a characteristic time constant $\tau_{e\text{-ph}}=C_e/G_{e\text{-ph}}$ associated with the electron system. Standard bolometer theory[10,11] predicts a frequency dependence of the device impedance $Z\equiv dV/dI$:

$$Z(\omega)=R\frac{1+\dfrac{P\alpha}{G_{e\text{-ph}}T_e}+j\omega\tau_{e\text{-ph}}}{1-\dfrac{P\alpha}{G_{e\text{-ph}}T_e}+j\omega\tau_{e\text{-ph}}}=Z_0\frac{1+j\omega\tau_{e\text{-ph}}\dfrac{Z_0+R}{2Z_0}}{1+j\omega\tau_{e\text{-ph}}\dfrac{Z_0+R}{2R}},\qquad(5)$$

where $\alpha=d\ln R/d\ln T$ is the thermometer sensitivity, $\tau_{e\text{-ph}}=C_e/G_{e\text{-ph}}$ is the thermal time constant, and

$$Z_0=Z(\omega=0)=R\frac{1+\dfrac{P\alpha}{G_{e\text{-ph}}T_e}}{1-\dfrac{P\alpha}{G_{e\text{-ph}}T_e}}.\qquad(6)$$

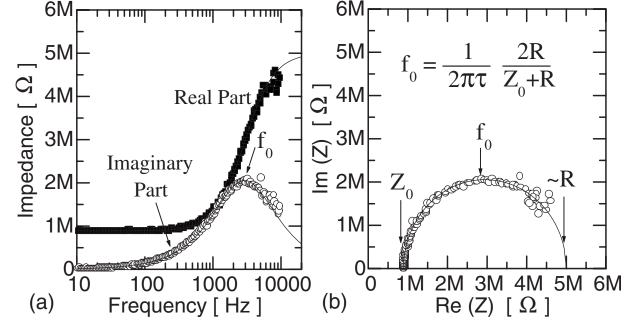

FIG. 2. Typical impedance as a function of frequency for a thermistor cemented directly to the heat sink. (a) Re[$Z(\omega)$] and Im[$Z(\omega)$] versus ω, (b) Im[$Z(\omega)$] versus Re[$Z(\omega)$]. The solid line is the fit using Eq. (5). For this device the net doping density is 2.45×10^{18} cm^{-3}. The data have been acquired at a heat sink temperature of 80 mK and a bias power of 1.5×10^{-12} W.

At low frequencies, the impedance must simply follow the local slope of the I-V curve, i.e., $Z(0)=dV/dI$, while for $\omega\gg1/\tau_{e\text{-ph}}$, the temperature and therefore the resistance will not change appreciably, and $Z=R(\equiv V/I)$. At intermediate frequencies, there will be a phase shift, and the impedance should follow a semicircle in the complex plane,[10] as shown in Fig. 2.

We measure $Z(\omega)$ by adding a small ac voltage to the dc bias voltage at the top of the load resistor and observing the relative magnitude and phase of the voltage across the thermistor. Details of the technique and the information provided by $Z(\omega)$ can be found in Vaillancourt.[17] Improved methods for correcting for stray circuit impedances that allow good measurements to be made up to higher frequencies are given in Lindeman *et al.*[18]

In these measurements, we find the high-frequency limiting value of $Z(\omega)$ to be systematically somewhat less that R. This is expected if there is an additional nonlinearity that has a much shorter characteristic time than $\tau_{e\text{-ph}}$.[11,19] Earlier studies of nonlinearity in *VRH* conductivity have found that there are regimes of doping density and temperature where the standard exponential field-dependence models fit well over a wide range of field values, other regimes where the hot-electron model fits very well, and intermediate areas where both effects must be included.[4,20] It seems reasonable that both effects always exist, but dominate under different conditions. Measurements of $Z(\omega)$ should provide a better way to separate these effects than simply observing the functional form of the nonlinearity with applied field or power density as long as the characteristic time scales are very different. The time scales associated with *VRH* field dependence should be much shorter than those observed here. We have not investigated an adequate range of doping densities to verify the postulated behavior. For the present range of interest, the apparent field effects are small and do not appreciably affect the derived values.

We have measured $R(T_{\text{sink}},P)$ and $Z(\omega)$ for a number of devices cemented directly to a heat sink (see, e.g., Figs. 1 and 2). We find good fits to the hot-electron model for both quantities, and can use the fitted values of $\tau_{e\text{-ph}}$ and $G_{e\text{-ph}}$ to find the apparent C_e at each temperature.

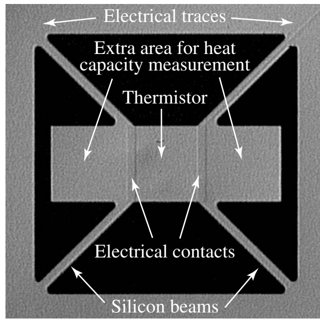

FIG. 3. Photo of a free standing device used to measure the heat capacity of the implanted region. This device has a central thermistor suspended on four silicon beams. The electrical signal from the thermistor is read out through degenerate contact implants and two traces of shallow degenerate implant that do not contribute appreciably to the thermal conductivity. The extra $120 \times 120\ \mu\mathrm{m}^2$ "wings" can be undoped or doped silicon. The difference between the total heat capacity in the two cases is used to estimate the heat capacity of the impurity system in the doped wings. The central thermistor has the same geometry as the ones used in the $G_{e\text{-ph}}$ and C_e measurements, but in those cases it was not isolated from the thick backing or "handle" wafer.

We also made independent measurements of the total heat capacity of the impurity system using isolated structures on the same silicon dice that contained the heat sunk devices used above. These monolithic structures contained a doped region used as a thermometer with extra silicon areas next to it, with the combined structure isolated on thin silicon beams (see Fig. 3). The thermal conductivity of the silicon support beams was measured by fitting *I-V* or *R* vs *P* curves for the thermistor similarly to what has been done for Fig. 1. The beams were assumed to have conductivity of the form $G = G_0 T^{\beta}$, while the electron-phonon conductivity was calculated using parameters fixed by analyzing the *I-V* curves of an identical thermistor tied directly to the heat sink as in Sec. III. This could be combined with measurements of the dynamic impedance $Z(\omega)$ to determine the total heat capacity. The suspended devices were measured in pairs, where the only difference between the pair was that in one the additional areas were pure silicon, and in the other they contained the same doping as the thermometer. The difference in total heat capacity for these devices was taken to be the heat capacity of the impurity system for the added doped regions.

Both measurements of heat capacity were normalized to the doped volume and plotted against temperature in Fig. 4. The hot-electron measurements of different devices at various temperatures and bias conditions are consistent with each other and show no significant dependence on doping density over the small range observed. The hot-electron heat capacity is essentially identical to the total excess heat capacity of the impurity system measured on the suspended devices, with differences less than the measurement uncertainties. It is not obvious that one should expect the entire heat capacity of the impurity system to be coupled to the conducting electrons, but this seems to be the case, as was also observed by Marnieros *et al.*[9] for amorphous $\mathrm{Nb}_x\mathrm{Si}_{1-x}$. The temperature dependence is quite flat below 0.1 K and steepens to about $T^{0.6}$ between 0.1 and 0.2 K. A less-than-

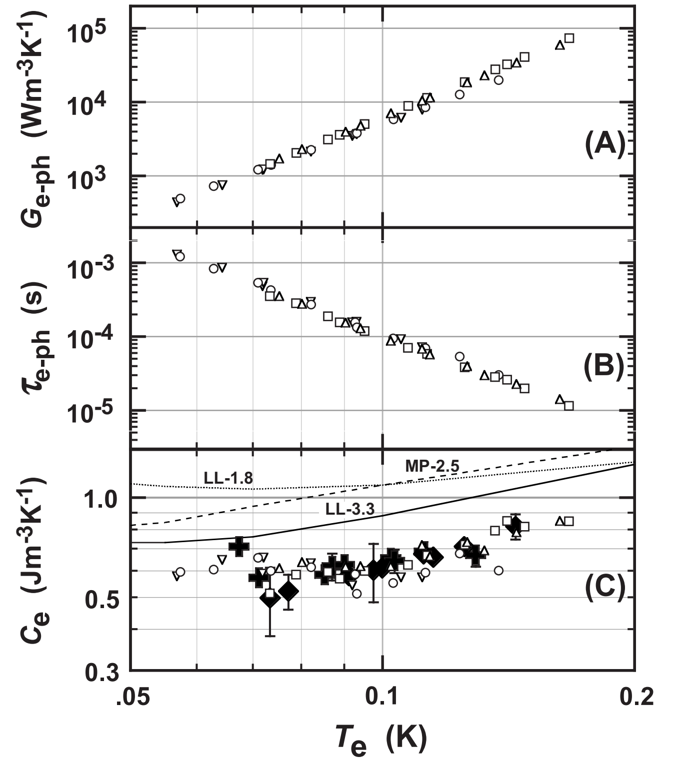

FIG. 4. Measurements of ion implanted and diffused Si:P:B devices with net doping densities ranging from $2.5 \times 10^{18}\ \mathrm{cm}^{-3}$ to $2.7 \times 10^{18}\ \mathrm{cm}^{-3}$ and 50% compensation ($T_0 \approx 6-11$ K), as a function of electron temperature T_e. (A) Apparent thermal conductivity $G_{e\text{-ph}}$ determined from *R* vs *P* curves (Sec. III). (B) Time constant determined from frequency dependence of complex impedance measurements (Sec. IV). (C) Open symbols are the product of (A) and (B), which corresponds to the electronic heat capacity in a hot electron description of the system. The filled symbols are the result of a "conventional" measurement of the total heat capacity introduced by the impurity system (see Fig. 3 and text). Different symbols correspond to different devices. For comparison, the lines show published data for total impurity heat capacity for uncompensated Si:P at similar donor densities $1.8 \times 10^{18}\ \mathrm{cm}^{-3}$ (LL-1.8) (Ref. 22), $3.3 \times 10^{18}\ \mathrm{cm}^{-3}$ (LL-3.3) (Ref. 22), and $2.5 \times 10^{18}\ \mathrm{cm}^{-3}$ (MP-2.5) (Ref. 23).

linear temperature dependence is expected theoretically due to the presence of spin-exchange-coupled clusters.[21] Very similar temperature dependences with absolute values of *C* about 35% higher have been measured for uncompensated Si:P (Refs. 22 and 23) (see Fig. 4). The difference in magnitude could be due to our measurement of 50% compensated Si:P:B versus their measurement of uncompensated Si:P, although we do not know of any simple argument to suggest this.

V. THERMAL NOISE DUE TO THE DECOUPLING BETWEEN ELECTRONS AND PHONONS

Pressing the hot-electron picture yet further, we would expect fluctuations in the energy content of the electron system due to random transport of energy between it and the lattice.[11] For a thermistor tied directly to the heat sink, the

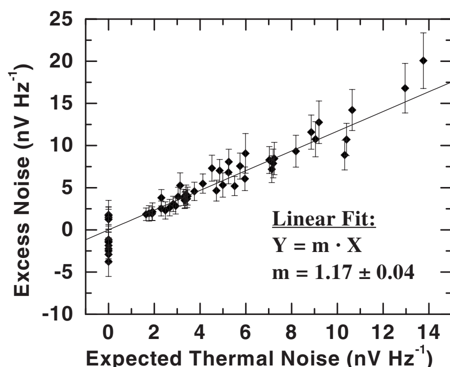

FIG. 5. Observed excess white noise in biased Si thermistors cemented directly to a heat sink versus the expected signal from thermodynamic fluctuations between the electron and phonon systems. Calculated Johnson noise has been subtracted from both.

magnitude of the transported power density spectrum should be $\sqrt{4k_BT^2G_{e\text{-ph}}}W/\sqrt{Hz}$, with small corrections for the steady-state temperature difference between the electrons and lattice.[24] In the low frequency limit, the relative temperature fluctuations depend only on $G_{e\text{-ph}}$, which is determined from the observed $R(T_{\text{sink}},P)$. The transduced response to these temperature fluctuations can be calculated from standard bolometer theory[10,11] and results in a white spectrum in the limit of low frequencies. This excess noise and the thermistor Johnson noise are both affected by electrothermal feedback,[11] so the relative magnitude of the load resistor must be taken into account. A derivation of this spectrum and the feedback corrections can be found in Galeazzi *et al.* and McCammon.[11,25]

To test this hypothesis, we made noise measurements on heat-sunk thermistors that are biased through 90 MΩ load resistors mounted on the ADR cold stage. The noise spectrum is measured at the output of the amplifier using a real time spectrum analyzer. The results show a white noise component in excess of the Johnson noise. This excess is plotted in Fig. 5 as a function of the calculated noise expected from these thermodynamic fluctuations, for a wide variety of bias currents and temperatures. There is rather good agreement with the predictions of the hot-electron model.

To verify that the apparent excess was not simply due to an underestimate of the Johnson noise, we have plotted our measured excess against the calculated Johnson noise after corrections for least resistor effect and electrothermal feedback. As shown in Fig. 6, there is little correlation between the measured excess and the expected Johnson noise, consistent with their having independent origins.

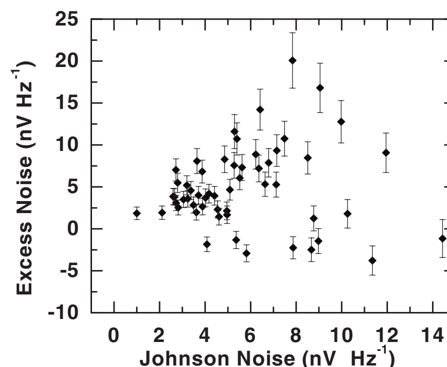

FIG. 6. Excess white noise in Si thermistors (see Fig. 5) versus the calculated Johnson noise.

VI. CONCLUSIONS

We have investigated the non-Ohmic behavior of doped Si at temperatures of 0.05–1 K. The results strongly support the existence of an electron temperature established by direct electron-electron interactions in strongly localized Si:P:B, analogous to the hot-electron effect in metals. In particular, we measured the dependence of the device resistance on the bias power, the time constant associated with the non-Ohmic behavior of the devices (that in the hot-electron picture leads to the electron heat capacity), and the excess noise deriving from power fluctuations in the thermal link between electrons and phonons. All of these quantities agree well with the predictions of the hot electron model over a wide range of temperatures and power density. If we accept the direct measurements of the heat capacity of the electron system, there are only two free parameters used for all the data: G_0 and β for the electron-phonon thermal conductance. These results provide strong quantitative support for the physical validity of the hot-electron model and seem to indicate that direct electron-electron interactions can dominate electron-phonon interactions in 3D *VRH* conductivity.

ACKNOWLEDGMENT

This work was supported in part by NASA Grant No. NAG5-629.

*Present address: Department of Physics, University of Miami, P.O. Box 248046, Coral Gables, FL 33124, USA; galeazzi@physics.miami.edu

[1] R. M. Hill, Philos. Mag. **24**, 1307 (1971).
[2] B. I. Shklovskii, Sov. Phys. Semicond. **10**, 855 (1976).
[3] N. Wang, F. C. Wellstood, B. Sadoulet, E. E. Haller, and J. Beeman, Phys. Rev. B **41**, 3761 (1990).
[4] J. Zhang, W. Cui, M. Juda, D. McCammon, R. L. Kelley, S. H. Moseley, C. K. Stahle, and A. E. Szymkowiak, Phys. Rev. B **57**, 4472 (1998).
[5] M. E. Gershenson, Yu. B. Khavin, D. Reuter, P. Schafmeister, and A. D. Wieck, Phys. Rev. Lett. **85**, 1718 (2000).
[6] R. Leturcq, D. L'Hote, R. Tourbot, V. Senz, U. Gennser, T. Ihn, K. Ensslin, G. Dehlinger, and D. Grutzmacher, Europhys. Lett. **61**, 499 (2003).
[7] G. M. Minkov, A. A. Sherstobitov, O. E. Rut, and A. V. Ger-

manenko, Physica E (Amsterdam) **25**, 42 (2004).
[8] G. M. Minkov, A. V. Germanenko, O. E. Rut, A. A. Sherstobitov, and B. N. Zvonkov, Phys. Rev. B **75**, 235316 (2007).
[9] S. Marnieros, L. Berge, A. Juillard, and L. Dumoulin, Phys. Rev. Lett. **84**, 2469 (2000).
[10] J. C. Mather, Appl. Opt. **21**, 1125 (1982).
[11] M. Galeazzi and D. McCammon, J. Appl. Phys. **93**, 4856 (2003).
[12] M. Galeazzi, K. R. Boyce, R. Brekosky, J. D. Gygax, R. L. Kelley, D. Liu, D. McCammon, D. B. Mott, F. S. Porter, W. T. Sanders, C. K. Stahle, C. M. Stahle, A. E. Szymkowiak, and P. Tan, in *Low Temperature Detectors: Ninth International Workshop on Low Temperature Detectors*, edited by F. S. Porter, D. McCammon, M. Galeazzi, and C. K. Stahle, AIP Conf. Proc. No. 605 (AIP, Melville, NY, 2002), p. 83.
[13] R. P. Brekosky, C. A. Allen, M. Galeazzi, J. D. Gygax, H. Isenburg, R. L. Kelley, D. McCammon, R. A. McClanahan, F. S. Porter, C. K. Stahle, and A. E. Szymkowiak, Nucl. Instrum. Methods Phys. Res. A **520**, 439 (2004).
[14] D. McCammon, in *Cryogenic Particle Detection*, edited by C. Enss, Topics in Applied Physics No. 99 (Springer, Berlin, 2005), p. 35.
[15] D. McCammon, R. Almy, E. Apodaca, W. Bergmann Tiest, W. Cui, S. Deiker, M. Galeazzi, M. Juda, A. Lesser, W. T. Sanders, J. Zhang, E. Figueroa-Feliciano, R. L. Kelley, S. H. Moseley, R. F. Mushotzky, F. S. Porter, C. K. Stahle, and A. E. Szymkowiak, Astrophys. J. **576**, 188 (2002).
[16] J. Zhang, W. Cui, M. Juda, D. McCammon, R. L. Kelley, S. H. Moseley, C. K. Stahle, and A. E. Szymkowiak, Phys. Rev. B **48**, 2312 (1993).
[17] J. E. Vaillancourt, Rev. Sci. Instrum. **76**, 043107 (2005).
[18] M. A. Lindeman, K. A. Barger, D. E. Brandl, S. G. Crowder, L. Rocks, and D. McCammon, Rev. Sci. Instrum. **78**, 043105 (2007).
[19] J. C. Mather, Appl. Opt. **23**, 584 (1984).
[20] M. Piat, J. P. Torre, J. W. Beeman, J. M. Lamarre, and R. S. Bhatia, J. Low Temp. Phys. **125**, 189 (2001).
[21] R. N. Bhatt and P. A. Lee, Phys. Rev. Lett. **48**, 344 (1982).
[22] M. Lakner and H. v. Löhneysen, Phys. Rev. Lett. **63**, 648 (1989).
[23] M. A. Paalanen, J. E. Graebner, R. N. Bhatt, and S. Sachdev, Phys. Rev. Lett. **61**, 597 (1988).
[24] W. S. Boyle and K. F. Rodgers, J. Opt. Soc. Am. **49**, 66 (1959).
[25] D. McCammon, in *Cryogenic Particle Detection*, edited by C. Enss, Topics in Applied Physics No. 99 (Springer, Berlin, 2005), p. 1.